



Predictive value of change in percent calcified plaque burden based on serial coronary computed tomographic angiography for cardiovascular events

Wei Wu^{1#}, Xi-Xia Sun^{1#}, Yao Pan¹, Ya-Qi Gao¹, Ya-Na Dou², Yue-Peng Zhang¹, Shuang Pan¹, Hao Wang¹, Zhao-Qian Wang¹, Chong-Fu Jia¹

¹Department of Cardiovascular Radiology, The First Affiliated Hospital of Dalian Medical University, Dalian, China; ²Siemens Healthineers Ltd., Beijing, China

Contributions: (I) Conception and design: CF Jia, XX Sun, W Wu; (II) Administrative support: None; (III) Provision of study materials or patients: Y Pan, YQ Gao, S Pan, YP Zhang; (IV) Collection and assembly of data: YN Dou, W Wu, H Wang; (V) Data analysis and interpretation: CF Jia, ZQ Wang, W Wu; (VI) Manuscript writing: All authors; (VII) Final approval of manuscript: All authors.

[#]These authors contributed equally to this work.

Correspondence to: Dr. Chong-Fu Jia, MD. Department of Cardiovascular Radiology, The First Affiliated Hospital of Dalian Medical University, No. 222, Zhongshan Road, Dalian 116011, China. Email: chongfujia@sina.com.

Background: Plaque progression is an independent risk factor for major adverse cardiovascular events (MACE), and change in the total plaque burden (PB) is a common indicator of plaque progression. However, the type of component (calcification or non-calcification) and the magnitude of changes cannot be determined. We aimed to analyze the capability of the percent calcified PB (PCPB) in reflecting the total and its noncalcified and calcified component PB change, and the predictive value of PCPB for MACE.

Methods: Patients who received two or more coronary computed tomographic angiography (CCTA) examinations were included and were divided into MACE and non-MACE groups. The volumes of total plaque, subcomponents and vessel were measured in the serial CCTA. The segmental stenosis score (SSS), high-risk plaque (HRP), total and subcomponent PB, and their annual changes (Δ PB/year) were calculated. PCPB was calculated as (calcified PB/total PB) \times 100%.

Results: Totally 116 patients were enrolled in this study, including 26 (22.4%) patients with MACE. The Δ PCPB/year showed negative correlation with Δ total PB/year ($r=-0.353$, $P<0.001$), Δ noncalcified PB/year ($r=-0.591$, $P<0.001$), while positively correlated with Δ calcified PB/year ($r=0.400$, $P<0.001$). If the Δ PCPB/year covariate was not added, the baseline HRP, Framingham risk score (FRS), and Δ total PB/year were independent predictors of MACE. Otherwise, the HRP_{baseline}, FRS_{baseline}, and Δ PCPB/year became independent risk factors of MACE. The area under the curve (AUC) of HRP_{baseline} + FRS_{baseline} + Δ PCPB/year was higher than that of HRP_{baseline} + FRS_{baseline} + Δ total PB/year (AUC: 0.894 vs. 0.820, $P=0.016$).

Conclusions: The Δ PCPB/year index simultaneously reflects changes of the total and its internal compositions PB. Moreover, our study shows the potential of Δ PCPB/year to predict MACE independently from the annual change of total PB.

Keywords: Coronary artery; atherosclerosis; serial coronary computed tomographic angiography (serial CCTA); adverse cardiovascular events

Submitted Sep 01, 2024. Accepted for publication Mar 06, 2025. Published online Mar 28, 2025.

doi: 10.21037/qims-24-1846

View this article at: <https://dx.doi.org/10.21037/qims-24-1846>

Introduction

Several studies have reported that plaque progression is an intermediate link and independent risk factor for the evolution of coronary artery lesions into cardiac events (1-3), and changes in total plaque burden (PB) based on coronary computed tomographic angiography (CCTA) constitute a common indicator of plaque progression (4). However, the total PB cannot reflect which composition (calcification or noncalcification) progresses and their magnitudes, and calcified and noncalcified plaque progression have considerably different predictive values for major adverse cardiovascular events (MACE) (5-10). The progression of the coronary artery calcium score has negligible effect on future risk prediction (5,6), and preventative treatments such as statins can increase calcification, however, it reduces the risk of MACE (7,8). Unlike calcification, the progression of the noncalcified composition is associated with a higher incidence of MACE (9,10). Therefore, finding a new indicator that reflects the evolution of the total and its internal compositions PB simultaneously will be of great value in accurately predicting MACE.

Unlike noncalcification plaque formation, coronary artery calcification is an irreversible lesion, that is to say, calcification can only remain unchanged or increase with time but cannot be reversed (11,12). Based on the above characteristics of calcification and the division algorithm (the relationship between dividend, divisor and quotient), this study proposed that changes in the new index of calcified PB to total PB, termed as the percent calcified PB (PCPB), over time simultaneously reflects the total and its noncalcified and calcified composition PB change. We aimed to verify this hypothesis and explore the predictive value of PCPB dynamic change for MACE. We present this article in accordance with the STROBE reporting checklist (available at <https://qims.amegroups.com/article/view/10.21037/qims-24-1846/rc>).

Methods

Study population

From May 2016 to August 2022, consecutive patients who received more than once CCTA examinations in The First Affiliated Hospital of Dalian Medical University were retrospectively included. Inclusion criteria were as follows: (I) the interval between the two CCTA examinations was >1 year; and (II) coronary artery lesions existed at the baseline CCTA with some calcified compositions. Patients

were excluded from the study for the following reasons: (I) poor image quality (discontinued image or poor contrast filling, etc.); (II) myocardial infarction detected before follow-up CCTA examination; (III) percutaneous coronary intervention (PCI) or coronary artery bypass grafting (CABG) before or within 3 months after the follow-up CCTA examination; or (IV) incomplete clinical data or lost to follow-up. Within 1 week before or after the baseline CCTA examination, the general data of all subjects were collected, and blood pressure measurement and blood collection were performed. Framingham risk score (FRS) was calculated to estimate the 10-year risk of coronary heart disease. MACE was defined as cardiac death, nonfatal myocardial infarction (ST-segment elevation and non-ST-segment elevation), and PCI or CABG was performed after follow-up CCTA (>3 months). The follow-up was conducted through on-site inquiry, electronic medical records, telephone calls, and emails. The last follow-up was in May 2023. The study was conducted in accordance with the Declaration of Helsinki (as revised in 2013). The study was approved by the Ethics Committee of The First Affiliated Hospital of Dalian Medical University (No. PJ/79-11/2019/XJS), and all patients signed an informed consent form. The research flowchart is shown in *Figure 1*.

CCTA examination

Siemens third-generation dual-source computed tomographic (CT) (Somatom Force, Siemens Medical Solutions, Forchheim, Germany) was used. All patients were given sublingual nitroglycerin 0.25 mg (AstraZeneca Pharma, Wuxi, China) 5 minutes before CCTA. Contrast agent (iohexol 300 mg/mL) was injected through the antecubital vein with a German Ulrich (Ulm, Germany) double-barreled high-pressure syringe; 40–55 and 20–35 mL were injected in the first and second phases, at flow rates of 5.0–5.5 and 3.5–4.0 mL/s, respectively. In the third phase, 30 mL of normal saline was injected at a flow rate of 4.0 mL/s. When the region of interest placed at the level of the ascending aorta had a CT value of 100 Hounsfield unit (HU), the scan was automatically triggered by a delay of 5 seconds. The prospective scanning mode was used, the tube voltage (120 or 100 kV) was adjusted according to body mass index, and current were automatically modulated using CareDose 4D. The remaining scan parameters were: rotation speed: 0.28 s/r, detector collimation: 2 mm × 96 mm × 0.6 mm, slice thickness: 0.75 mm, slice interval: 0.7 mm and convolution kernel Bv 40 (strength 3).

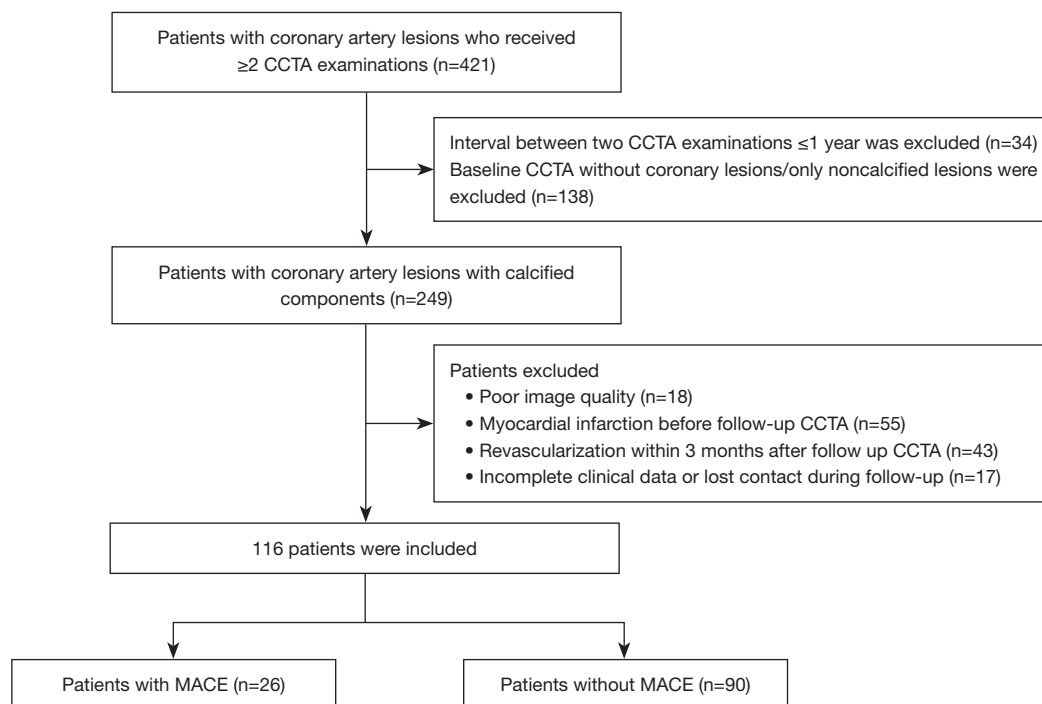


Figure 1 Flow chart of the study. CCTA, coronary computed tomographic angiography; MACE, major adverse cardiovascular events.

CCTA image measurement and analysis

Coronary arteries with a diameter ≥ 1.5 mm were analyzed using semi-automatic plaque analysis software (Coronary Plaque Analysis 5.0.1 syngo.via FRONTIER, Siemens Healthineers, Beijing, China), and manual adjustments were made when necessary. Plaque volumes (mm^3) were calculated for each coronary lesion and then summated to compute the total plaque volume at the patient level. Plaque volume was categorized using HU ranges (13): low attenuation (-30 to 30 HU), fibro-fatty (30 to 130 HU), fibrous (131 to 350 HU), and calcified plaque (>350 HU). The segmental stenosis score (SSS) was defined as the sum of the stenosis degree of the involved coronary segments, and the change in SSS (ΔSSS) was calculated as $\text{SSS}_{\text{follow-up}} - \text{SSS}_{\text{baseline}}$. Plaque with ≥ 2 high-risk features was defined as high-risk plaque (HRP), high-risk features included (13): (I) positive remodeling (remodeling index >1.1), remodeling index: diameter of blood vessels at the lesion/[sum of diameters of normal blood vessels in the proximal and distal parts of the lesion]/2; (II) low-attenuation plaque: CT value of any voxel of the plaque <30 HU; (III) spotty calcification: the largest diameter of the calcification in any direction <3 mm; and (IV) napkin ring sign: the circular

high-attenuation area enclosed the low-attenuation plaque core and had CT value ≤ 130 HU.

PB was calculated as (plaque volume/vessel volume) $\times 100\%$, the vessel volume is defined as the volume of all coronary segments regardless of whether they contain plaque or not. Longitudinal analysis of changes in PB was calculated as annualized rates to account for the variability in time between baseline and follow-up CCTA. the annual change in PB ($\Delta\text{PB}/\text{year}$) = $(\text{PB}_{\text{follow-up}} - \text{PB}_{\text{baseline}})/\text{interval}$ time between the two CCTAs. PCPB was calculated as (calcified PB/total PB) $\times 100\%$, and the annual change of PCPB ($\Delta\text{PCPB}/\text{year}$) = $(\text{PCPB}_{\text{follow-up}} - \text{PCPB}_{\text{baseline}})/\text{interval}$ time between the two CCTAs. The magnitude of change in PB was calculated as $(\Delta\text{PB}/\text{total PB}_{\text{baseline}}) \times 100\%$.

Statistical analysis

Statistical Package for the Social Sciences (SPSS) 26.0 (IBM Corp., Armonk, NY, USA) and Medcalc statistical software (Ostend, Belgium) were used for all statistical analyses. Continuous data were expressed as means \pm standard deviations, and categorical data were expressed as frequencies (n) or percentages (%). Continuous variables were compared using independent sample *t*-tests.

Table 1 Comparison of clinical features between the MACE and non-MACE groups

Characteristics	Total (n=116)	MACE (n=26)	Non-MACE (n=90)	P
Age, years	65.0±10.7	68.0±9.8	64.3±11.0	0.130
Gender (male)	79 (68.1)	19 (73.1)	60 (66.7)	0.358
BMI, kg/m ²	25.5 (23.4, 27.0)	23.9 (22.8, 26.4)	25.8 (23.7, 27.6)	0.036
CCTA interval, months	28±11	26±11	28±12	0.755
Follow-up time, months	60±13	61±14	60±13	0.768
Hypertension	59 (50.9)	15 (57.7)	44 (48.9)	0.285
Diabetes	27 (23.3)	7 (26.9)	20 (22.2)	0.397
Hyperlipidemia	75 (64.7)	20 (76.9)	55 (61.1)	0.103
CAD family history	8 (6.9)	1 (3.8)	7 (7.8)	0.428
Smoking history	36 (31.0)	9 (34.6)	27 (30.0)	0.412
Drinking history	35 (30.2)	9 (34.6)	26 (28.9)	0.630
Statin treatment	74 (63.8)	20 (76.9)	54 (60.0)	0.086
Aspirin treatment	61 (52.6)	14 (53.8)	47 (52.2)	0.531
β-blockers treatment	53 (45.7)	15 (57.7)	38 (42.2)	0.121
Total cholesterol, mmol/L	4.8±1.0	4.5±1.1	4.9±1.0	0.089
Triglycerides, mmol/L	1.4 (1.0, 2.2)	1.3 (0.8, 2.1)	1.4 (1.0, 2.2)	0.535
LDL, mmol/L	2.7±0.7	2.5±0.8	2.8±0.7	0.186
HDL, mmol/L	1.2±0.3	1.1±0.3	1.3±0.3	0.024
FRS	15.1±8.1	19.7±6.7	13.5±8.0	0.001

Values are the mean ± standard deviation, median (interquartile range), or n (%). BMI, body mass index; CAD, coronary artery disease; CCTA, coronary computed tomographic angiography; FRS, Framingham risk score; HDL, high-density lipoprotein; LDL, low-density lipoprotein; MACE, major adverse cardiac events.

Categorical data were compared using Chi-squared tests. Correlation analyses were conducted using Pearson or Spearman correlation tests. Independent predictors of MACE were analyzed using univariate and multivariate Cox stepwise regression (forward: likelihood ratio). Receiver operating characteristic (ROC) curves were used, and areas under the curve (AUCs) were compared using DeLong tests. The Kaplan-Meier analysis log-rank test was used to estimate the event-free survival curve between the two groups. A P value of <0.05 indicated a statistical difference.

Results

General information and plaque characteristics

This study included 116 patients with an average age of 65.0±10.7 years, 68.1% of whom were men. The CCTA

interval and clinical follow-up time were 28±11 and 60±13 months, respectively (*Table 1*). One hundred and nine patients have undergone CCTA at 100 kV and the same tube voltage was used for the baseline and second CCTA. MACE events occurred in 26 patients (22.4%), including 4 cases of cardiac death, 16 cases of PCI or CABG, and 6 cases of myocardial infarction. The baseline degree of CCTA stenosis was mild in 91 patients (78.4%), moderate in 20 patients (17.2%), and severe in 5 patients (4.3%). The CCTA lesions were observed in a single vessel in 36 patients (31.0%) and in ≥2 vessels in 80 patients (69.0%).

The baseline FRS and high-density lipoprotein (HDL) levels of the MACE group were significantly higher and lower than those of the non-MACE group, respectively (P<0.05). Total cholesterol, low-density lipoprotein (LDL), and HDL levels at baseline were higher than those at the second CCTA examination (4.8±1.0 *vs.* 4.5±1.1, P=0.042;

Table 2 Computed tomography features between the MACE and non-MACE groups

Variables	Total (n=116)	MACE (n=26)	Non-MACE (n=90)	P
Baseline				
HRP	18 (15.5)	8 (30.8)	10 (11.1)	0.027
SSS, n	4.0 (3.0, 7.0)	6.0 (4.0, 9.0)	4.0 (2.0, 6.0)	0.001
Total PB, %	32.1 (16.3, 56.0)	31.5 (20.1, 58.0)	32.4 (13.4, 55.2)	0.357
Noncalcified PB, %	17.0 (8.9, 37.1)	19.4 (14.1, 42.0)	13.4 (7.9, 33.3)	0.158
Low attenuation PB, %	0.1 (0.0, 0.7)	0.3 (0.0, 1.2)	0.1 (0.0, 0.6)	0.061
Fibro-fatty PB, %	3.7 (1.6, 9.7)	5.7 (2.5, 11.9)	3.4 (1.4, 8.3)	0.298
Fibrous PB, %	12.1 (5.7, 25.0)	12.8 (8.7, 27.0)	11.4 (4.9, 24.9)	0.330
Calcified PB, %	8.0 (1.8, 22.3)	10.1 (7.6, 23.8)	5.4 (1.1, 22.5)	0.062
PCPB, %	30.1 (9.7, 57.8)	32.3 (24.7, 45.6)	28.1 (7.2, 61.6)	0.185
Changes				
ΔHRP	15 (12.9)	5 (19.2)	10 (11.1)	0.377
ΔSSS, n	0.0 (0.0, 1.0)	0.0 (0.0, 0.5)	0.5 (0.0, 1.0)	0.074
ΔTotal PB/year, %/y	3.9 (1.6, 6.9)	5.6 (3.7, 11.7)	3.5 (1.3, 6.2)	0.001
ΔNoncalcified PB/year, %/y	1.8 (0.2, 4.5)	4.6 (2.1, 11.1)	1.3 (−0.1, 3.6)	<0.001
ΔLow attenuation PB/year, %/y	0.1 (0.0, 0.5)	0.4 (−0.1, 0.7)	0.1 (0.0, 0.4)	0.079
ΔFibro-fatty PB/year, %/y	0.7 (0.0, 3.0)	2.2 (0.7, 5.7)	0.5 (−0.3, 1.9)	0.001
ΔFibrous PB/year, %/y	0.7 (−0.4, 1.9)	1.3 (0.2, 2.9)	0.5 (−0.6, 1.7)	0.024
ΔCalcified PB/year, %/y	1.1 (0.2, 2.7)	0.8 (0.2, 2.5)	1.2 (0.3, 2.8)	0.183
ΔPCPB/year, %/y	0.7 (−1.2, 3.9)	−2.8 (−4.7, 0.3)	1.2 (−0.5, 5.4)	<0.001

Values are the median (interquartile range) or n (%). Δ, change between follow-up and baseline. HRP, high-risk plaque; MACE, major adverse cardiac events; PB, plaque burden; PCPB, percent calcified plaque burden; SSS, segmental stenosis score; y, year.

2.7±0.7 vs. 2.5±0.8, P=0.012; 1.2±0.3 vs. 1.1±0.3, P=0.010). The baseline HRP and SSS in the MACE group were significantly higher than that in the non-MACE group (P<0.05). The changes of total, fibro-fatty and fibrous PB/year but not calcified were higher in the MACE group than in the non-MACE group (P<0.05). ΔPCPB/year in the MACE group was lower than that in the non-MACE group (P<0.05), see *Table 2* and *Figures 2, 3*.

Association of ΔPCPB/year with CCTA characteristics and general information

The patients were divided into four groups according to the quartiles of ΔPCPB/year. As the quartiles increased, the baseline SSS, total PB, noncalcified PB, fibro-fatty PB, MACE incidence, Δtotal PB/year, Δnoncalcified PB/year, Δlow attenuation PB/year, Δfibro-fatty PB/year, and

Δfibrous PB/year decreased and the Δcalcified PB/year increased (P<0.05) (*Table 3* and *Figure 4*). No differences in other general information and CCTA characteristics were detected among the quartiles.

The ΔPCPB/year was negatively correlated with Δtotal PB/year, Δnoncalcified PB/year, Δlow attenuation PB/year, Δfibro-fatty PB/year, and Δfibrous PB/year (P<0.05) and positively correlated with the Δcalcified PB/year (P<0.001) (*Figure 5*). The changes in the noncalcified PB/year and calcified PB/year were 4.2% and 0.3% in the 52 patients with a ΔPCPB/year of <0, while they were 0.4% and 1.6% in the 64 patients with a ΔPCPB/year of >0, respectively.

Analysis of independent risk factors for MACE

Univariate Cox regression analysis was performed with the occurrence of MACE as the dependent variable, and

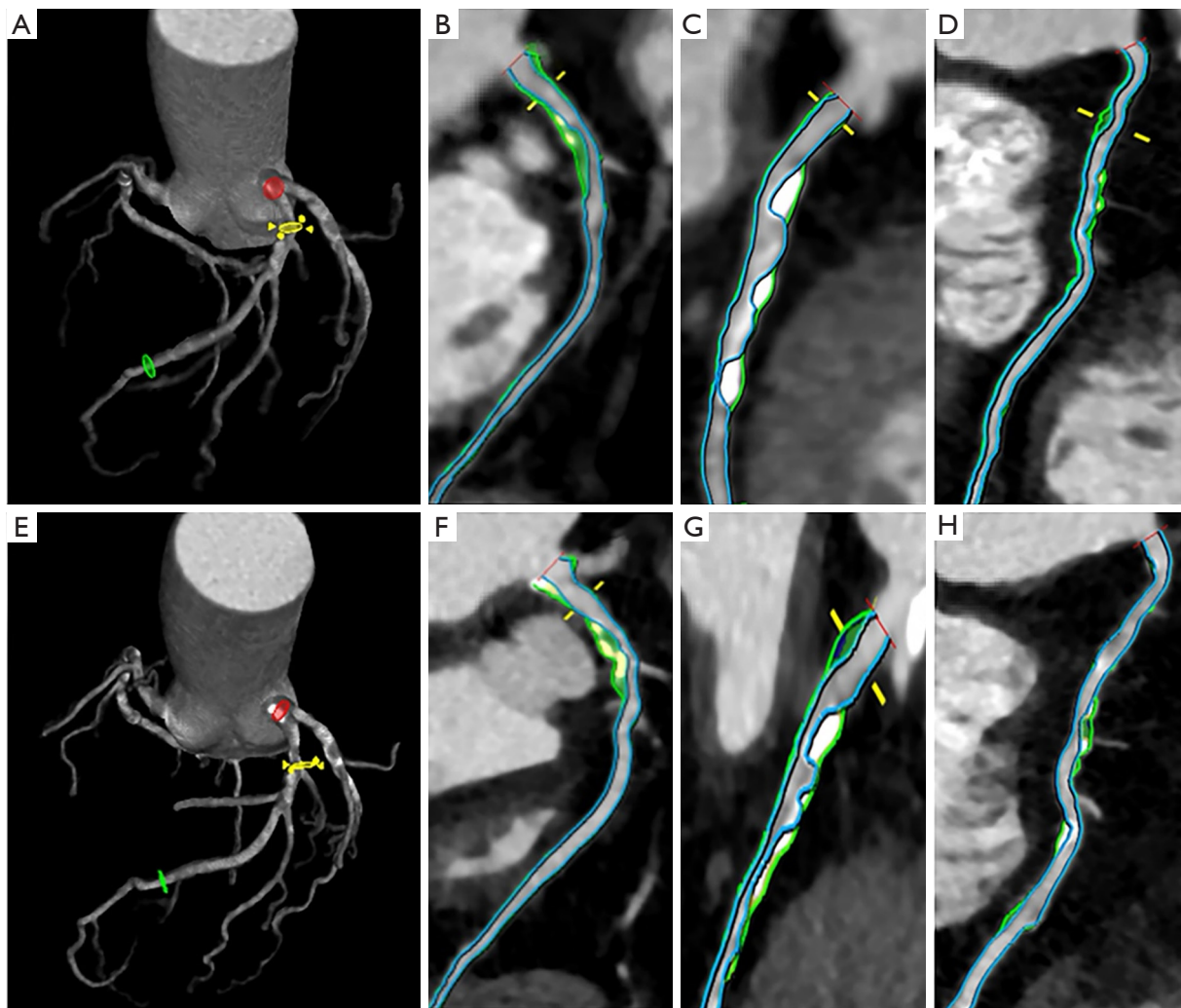


Figure 2 Baseline and follow-up CCTA reconstructed images of a 61-year-old woman without MACE. Baseline CCTA (A-D) showed mixed plaques in the left anterior descending, left circumflex, and right coronary arteries. The total, noncalcified, low attenuation, fibrous lipid, fibrous, and calcified PB were 107.4%, 78.6%, 1.4%, 18.5%, 58.7%, and 28.8%, respectively. The follow-up CCTA (E-H) showed the progression of total PB and enlargement of PCPB. The total, noncalcified, low attenuation, fibrous lipid, fibrous, and calcified PB were 118.8%, 74.0%, 5.0%, 26.7%, 42.3%, and 44.8%, respectively. The area outlined by the blue line is the coronary artery lumen, and the area between the green and blue lines is the coronary artery plaque. Yellow and white represent calcification and green represents noncalcification. CCTA, coronary computed tomographic angiography; MACE, major adverse cardiovascular event; PB, plaque burden; PCPB, percent calcified plaque burden.

clinical data and serial CCTA characteristics as covariates. Baseline characteristics (FRS, HDL, HRP, and SSS), and serial CCTA characteristics (Δ total PB/year, Δ fibrofatty PB/year, Δ fibrous PB/year, and Δ PCPB/year) were predictors of MACE, while Δ Calcified PB/year is not (Table 4).

Multivariate Cox regression analysis was carried out with

the occurrence of MACE as the dependent variable and the above-mentioned risk factors in univariate analysis as covariates. The results showed that $HRP_{baseline}$, $FRS_{baseline}$, and annual change of total PB were independent predictors of MACE. With the addition of the Δ PCPB/year covariate, $HRP_{baseline}$, $FRS_{baseline}$, and Δ PCPB/year became independent risk factors of MACE (Table 4).

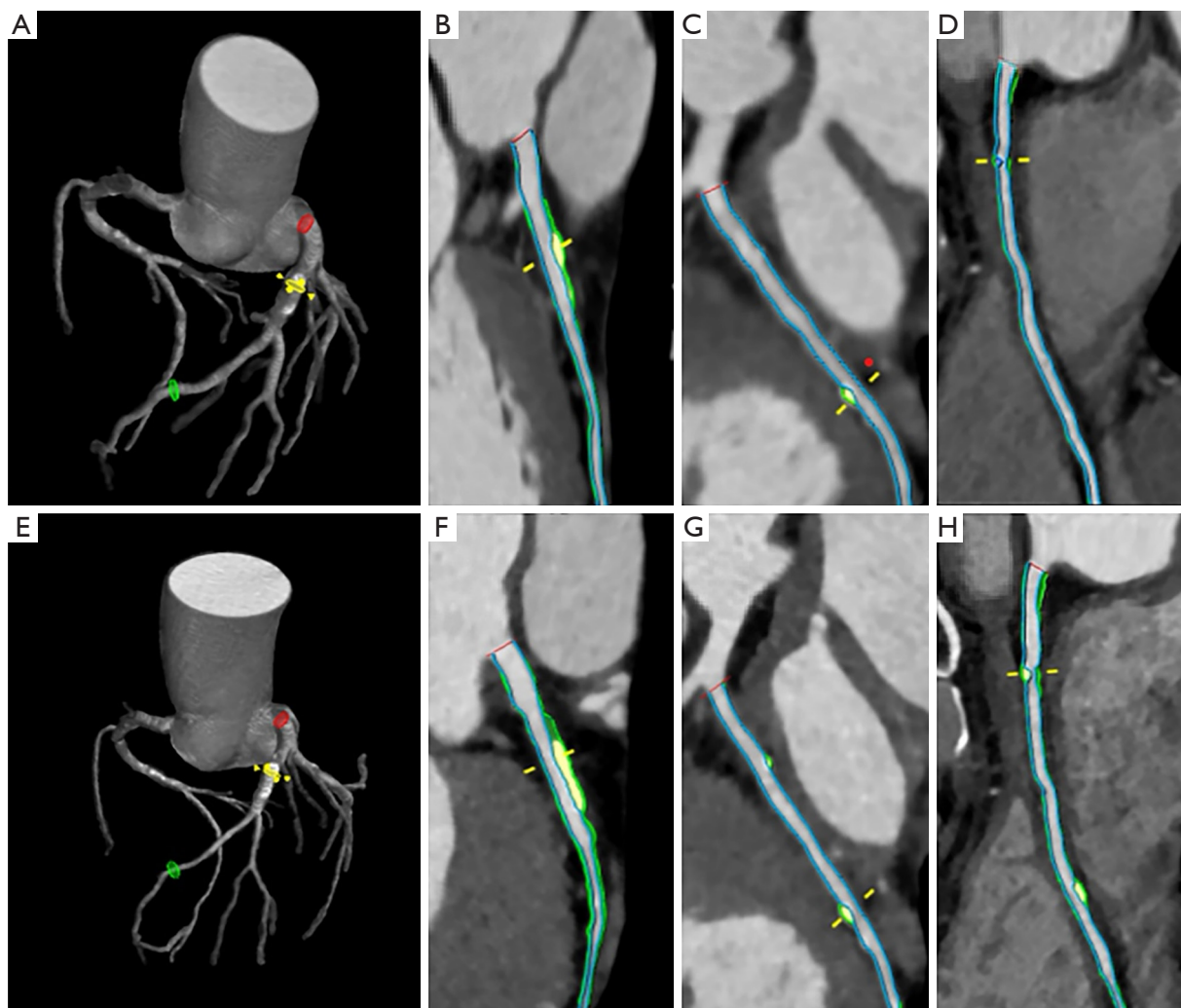


Figure 3 Baseline and follow-up CCTA reconstructed images of a 71-year-old man with MACE. Baseline CCTA (A-D) showed mixed plaques in the left anterior descending, left circumflex, and right coronary arteries. The total, noncalcified, low attenuation, fibro-fatty, fibrous, and calcified PB were 36.4%, 12.0%, 0.0%, 1.5%, 10.5%, and 24.4% respectively. Follow-up CCTA (E-H) showed the progression of the total PB and reduction of PCPB. The total, noncalcified, low attenuation, fibro-fatty, fibrous, and calcified PB were 62.0%, 32.0%, 1.0%, 15.8%, 15.2%, and 30.0%, respectively. The area outlined by the blue line is the coronary artery lumen, and the area between the green and blue lines is the coronary artery plaque. Yellow and white represent calcification and green represents noncalcification. CCTA, coronary computed tomographic angiography; MACE, major adverse cardiovascular event; PB, plaque burden; PCPB, percent calcified plaque burden.

Comparison of multiple MACE predictive models

The models of ROC curves were performed to evaluate the predictive value of single or combination of plaque parameters for MACE (Figure 6). In the univariate prediction model, the AUC of Δ PCPB/year was higher than that of baseline HRP, FRS and the annual change of total PB, although there were no significant differences. In the multivariate prediction model, the AUC of $\text{HRP}_{\text{baseline}}$

+ $\text{FRS}_{\text{baseline}}$ + Δ PCPB/year was significantly higher than that of $\text{HRP}_{\text{baseline}}$ + $\text{FRS}_{\text{baseline}}$ + annual change of total PB, and it was also significantly higher than that of any single predictor ($P < 0.05$). In ROC analysis, Δ PCPB/year $< -2.3\%$ showed a significant predictive value for adverse cardiac events [AUC: 0.809 (0.726–0.876), $P < 0.001$]. The Kaplan-Meier survival curves revealed a significantly worse cardiac outcome in patients with Δ PCPB/year $< -2.3\%$ (log-rank

Table 3 Comparison of general information and CCTA characteristics among the four groups categorized based on quartiles of Δ PCPB/year

Variables	Δ PCPB/year				P
	Group 1 (n=30)	Group 2 (n=30)	Group 3 (n=29)	Group 4 (n=30)	
Δ PCPB/year, %/y	-3.3 (-5.0, -2.3)	-0.3 (-0.7, -0.1)	1.9 (1.0, 2.6)	6.7 (5.4, 9.7)	<0.001
MACE	16 (55.2)	5 (17.2)	3 (17.2)	0 (0.0)	<0.001
Baseline					
HRP	5 (17.2)	4 (13.8)	10 (34.5)	1 (3.4)	0.017
SSS, n	6.0 (3.5, 8.5)	4.0 (2.0, 5.0)	5.0 (3.0, 7.0)	3.0 (2.0, 6.0)	0.047
Total PB, %	36.4 (23.4, 56.4)	29.3 (20.0, 57.4)	39.4 (20.1, 62.8)	16.2 (8.0, 47.4)	0.047
Noncalcified PB, %	17.1 (10.6, 37.4)	20.4 (8.6, 37.8)	29.6 (13.3, 41.1)	12.0 (6.4, 29.5)	0.057
Low attenuation PB, %	0.1 (0.0, 0.5)	0.2 (0.0, 0.9)	0.3 (0.1, 1.3)	0.6 (0.0, 2.6)	0.082
Fibro-fatty PB, %	3.9 (0.4, 9.5)	3.9 (1.4, 8.4)	7.2 (2.9, 12.4)	3.0 (1.6, 4.2)	0.055
Fibrous PB, %	10.7 (6.9, 26.2)	12.7 (4.9, 23.7)	19.1 (9.9, 26.1)	7.9 (3.7, 25.3)	0.209
Calcified PB, %	13.8 (8.2, 26.8)	7.7 (3.0, 24.2)	5.3 (2.6, 23.4)	3.0 (0.8, 19.1)	0.029
PCPB, %	36.6 (29.1, 67.1)	25.9 (1.4, 62.4)	15.7 (7.6, 55.2)	22.3 (9.4, 45.5)	0.048
Changes					
Δ HRP	6 (20.7)	3 (10.3)	-1 (-3.4)	2 (6.9)	0.145
Δ SSS, n	0.0 (0.0, 2.0)	0.0 (0.0, 2.0)	0.0 (0.0, 1.0)	0.0 (0.0, 1.0)	0.911
Δ Total PB/year, %/y	6.9 (4.0, 11.1)	3.9 (1.7, 6.3)	2.4 (0.9, 4.8)	1.9 (0.8, 5.9)	<0.001
Δ Noncalcified PB/year, %/y	5.0 (3.7, 10.7)	2.3 (1.3, 4.4)	0.9 (-0.8, 3.0)	-0.1 (-1.3, 0.8)	<0.001
Δ Low attenuation PB/year, %/y	0.2 (0.0, 0.6)	0.1 (0.0, 0.4)	0.2 (0.0, 1.0)	0.0 (-0.1, 0.1)	0.033
Δ Fibro-fatty PB/year, %/y	2.5 (0.3, 5.1)	1.5 (0.4, 3.8)	0.7 (-0.2, 1.9)	-0.3 (-1.0, 0.6)	<0.001
Δ Fibrous PB/year, %/y	2.3 (1.1, 4.5)	0.7 (-0.1, 1.6)	-0.1 (-1.1, 1.7)	-0.1 (-1.4, 0.9)	<0.001
Δ Calcified PB/year, %/y	0.3 (0.0, 2.1)	0.6 (0.0, 1.7)	1.6 (0.7, 2.3)	2.1 (1.2, 6.4)	<0.001

Values are the median (interquartile range) or n (%). The median values of Δ PCPB/year in groups 1 to 4 were -3.3%, -0.3%, 1.9%, and 6.7%, respectively. Δ , change between follow-up and baseline. HRP, high-risk plaque; MACE, major adverse cardiac events; PB, plaque burden; PCPB, percent calcified plaque burden; SSS, segmental stenosis score; y, year.

$P < 0.001$) (Figure 7).

Discussion

Comparing the clinical and serial CT features of patients with and without MACE in our study revealed the following findings: (I) Δ PCPB/year was negatively correlated with the annual changes of total PB and noncalcified PB, MACE incidence and positively correlated with the annual change of calcified PB; (II) the independent predictors of MACE were $HRP_{baseline}$, $FRS_{baseline}$ and annual change of total PB, however, with the addition of the Δ PCPB/year covariate, the independent predictors of MACE were $HRP_{baseline}$,

$FRS_{baseline}$, and Δ PCPB/year; (III) the AUC of $HRP_{baseline} + FRS_{baseline} + \Delta$ PCPB/year was higher than that of $HRP_{baseline} + FRS_{baseline} +$ annual change of total PB.

Our study showed that the Δ PCPB index can reflect the changes in both the total and its internal compositions PB. Furthermore, it can also reflect the magnitudes of changes in calcified and noncalcified compositions. The mechanism underlying this can be deduced based on the calculation formula of PCPB and the natural property of irreversible calcification. Bailey *et al.* (14) reported that calcification is irreversible owing to the imbalance of calcium and phosphorus concentrations in the lesion, resulting in the excessive deposition of calcium phosphate and formation

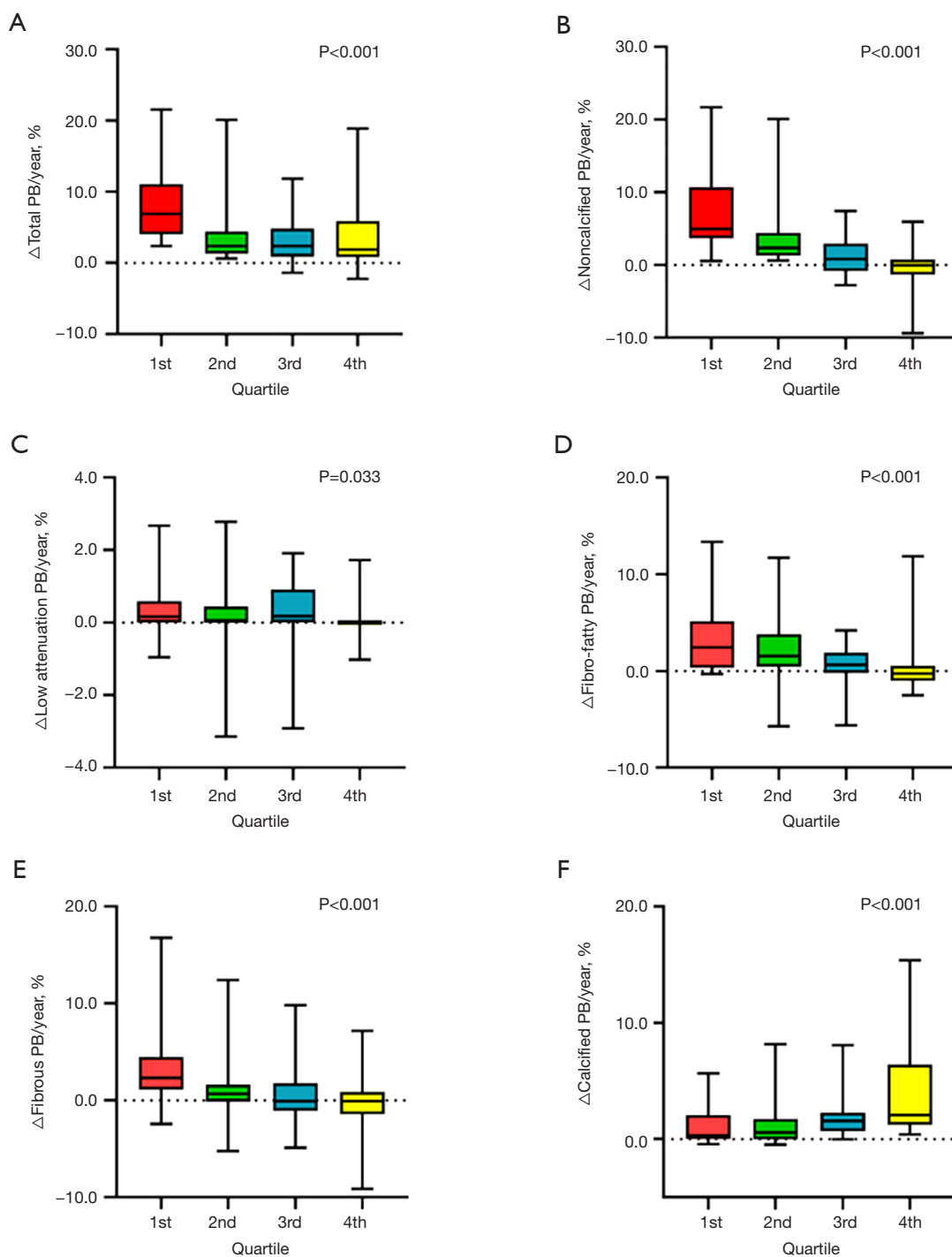


Figure 4 The annual changes of the total and internal compositions PB among the four groups categorized based on Δ PCPB/year. (A-E) Decreases in the Δ total PB/year, Δ noncalcified PB/year, Δ low attenuation PB/year, Δ fibro-fatty PB/year, and Δ fibrous PB/year, respectively, with increasing quartiles. (F) Increased calcified PB/year with increasing quartiles. The median values of Δ PCPB/year in groups 1–4 were –3.3%, –0.3%, 1.9%, and 6.7%, respectively. Δ , change between baseline and follow-up. PB, plaque burden; PCPB, percent calcified plaque burden.

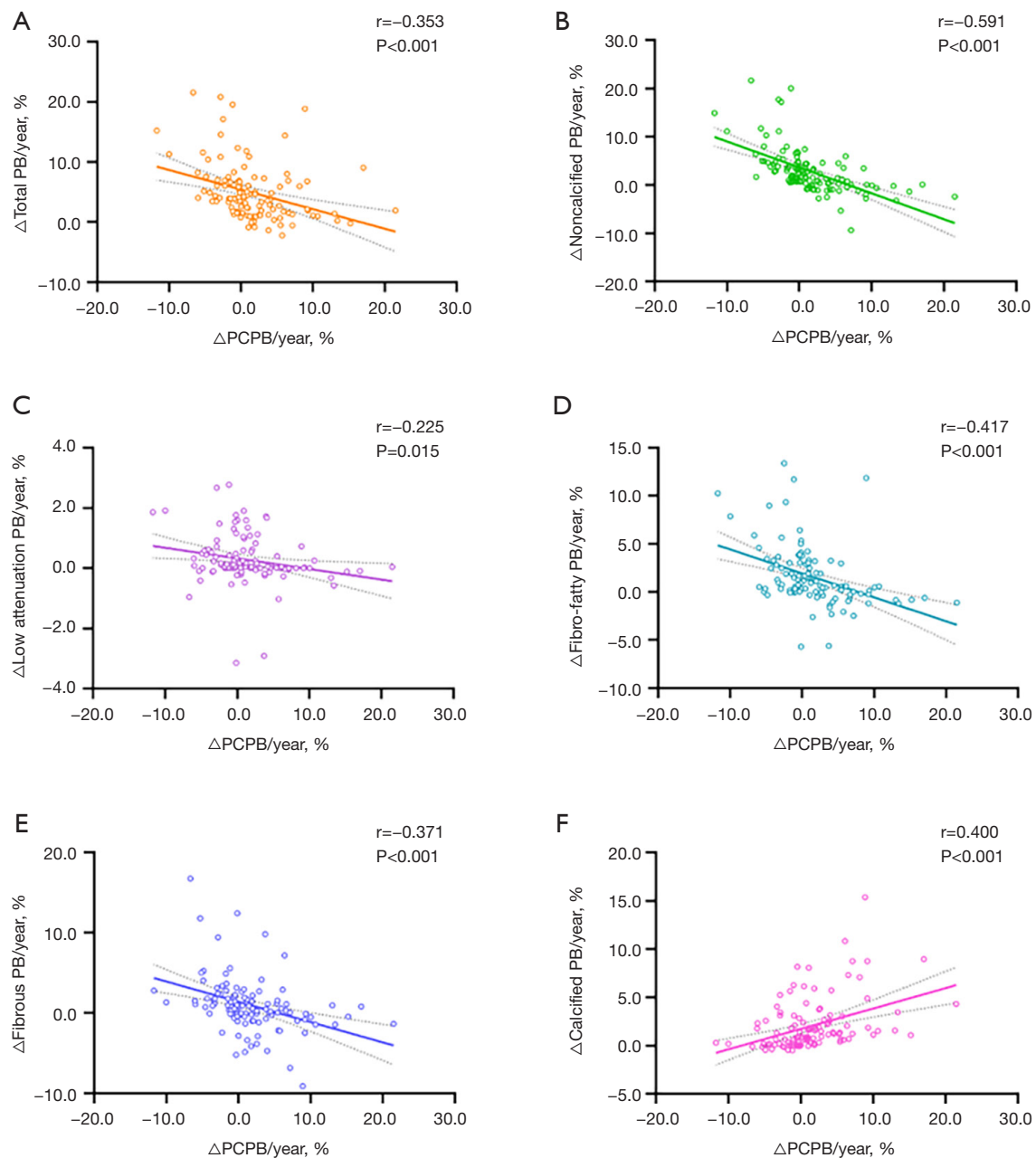


Figure 5 Correlation between $\Delta\text{PCPB}/\text{year}$ and the annual changes of total and the internal composition PB. (A-E) The annual changes of total PB, noncalcified PB, low attenuation PB, fibro-fatty PB, and fibrous PB were negatively correlated with $\Delta\text{PCPB}/\text{year}$ respectively; (F) the annual changes of calcified PB were positively correlated with $\Delta\text{PCPB}/\text{year}$. Δ , change between baseline and follow-up. PCPB, percent calcified plaque burden; PB, plaque burden.

of calcium phosphate crystals. According to the formula $\text{PCPB} = (\text{calcified PB}/\text{total PB}) \times 100\%$, the total PB (divisor) increases when PCPB (quotient) decreases because calcification (dividend) cannot decrease. Conversely, if PCPB increases, the increase of the total PB will be less

than the calcification. Our results verified this inference, the $\Delta\text{PCPB}/\text{year}$ was negatively correlated with the annual change of total PB, and with the increasing quartiles of $\Delta\text{PCPB}/\text{year}$, the annual change of total PB decreased.

Furthermore, we divided the total PB into calcification

Table 4 Univariate and multivariate Cox regression analysis of clinical data and CCTA characteristics

Predictors	Univariate		Multivariate	
	OR (95% CI)	P	OR (95% CI)	P
Age, years	1.029 (0.992–1.068)	0.128		
Gender (male)	0.786 (0.330–1.870)	0.586		
BMI	0.954 (0.885–1.028)	0.217		
Hypertension	1.455 (0.616–3.435)	0.392		
Diabetes	1.339 (0.550–3.258)	0.520		
Hyperlipidemia	2.556 (0.759–8.615)	0.130		
CAD family history	0.469 (0.063–3.479)	0.459		
Smoking history	1.244 (0.538–2.877)	0.609		
Drinking history	1.245 (0.539–2.876)	0.609		
Statin treatment	2.688 (0.798–9.054)	0.111		
Aspirin treatment	1.092 (0.472–2.525)	0.884		
β-blockers treatment	1.782 (0.755–4.207)	0.187		
Total cholesterol	0.689 (0.451–1.054)	0.086		
Triglycerides	0.831 (0.531–1.300)	0.417		
LDL	0.663 (0.359–1.224)	0.189		
HDL	0.192 (0.044–0.829)	0.027	1.008 (0.228–4.462)	0.992
FRS _{baseline}	1.100 (1.042–1.161)	0.001	1.087 (1.022–1.156)	0.008
HRP _{baseline}	3.556 (1.231–10.273)	0.019	4.126 (1.672–10.182)	0.002
SSS _{baseline}	1.199 (1.069–1.345)	0.002	1.011 (0.855–1.195)	0.899
Total PB _{baseline}	1.002 (0.991–1.014)	0.715		
Low attenuation PB _{baseline}	1.018 (0.992–1.045)	0.168		
Fibro-fatty PB _{baseline}	1.015 (0.967–1.066)	0.541		
Fibrous PB _{baseline}	1.013 (0.972–1.055)	0.545		
Calcified PB _{baseline}	0.999 (0.981–1.017)	0.903		
ΔHRP	1.186 (0.455–3.090)	0.727		
ΔSSS	0.807 (0.536–1.215)	0.304		
ΔTotal PB/year	1.119 (1.056–1.187)	<0.001	1.067 (1.067–1.137)**	0.048**
ΔLow attenuation PB/year	1.406 (0.890–2.221)	0.144		
ΔFibro-fatty PB/year	1.186 (1.083–1.298)	<0.001		
ΔFibrous PB/year	1.131 (1.037–1.234)	0.006		
ΔCalcified PB/year	0.891 (0.735–1.078)	0.235		
ΔPCPB/year	0.774 (0.703–0.852)	<0.001	0.744 (0.661–0.838)	<0.001

***ΔPCPB/year* has not been added. *ΔTotal PB/year* includes *Δfibro-fatty PB/year* and *Δfibrous PB/year* and has a linear relationship with them, so *Δtotal PB/year* was used for multivariate Cox regression analysis. *Δ*, change between follow-up and baseline. BMI, body mass index; CAD, coronary artery disease; CI, confidence interval; CCTA, coronary computed tomographic angiography; FRS, Framingham risk score; HDL, high-density lipoprotein; HRP, high-risk plaque; LDL, low-density lipoprotein; OR, odds ratio; PB, plaque burden; PCPB, percent calcified plaque burden; SSS, segmental stenosis score.

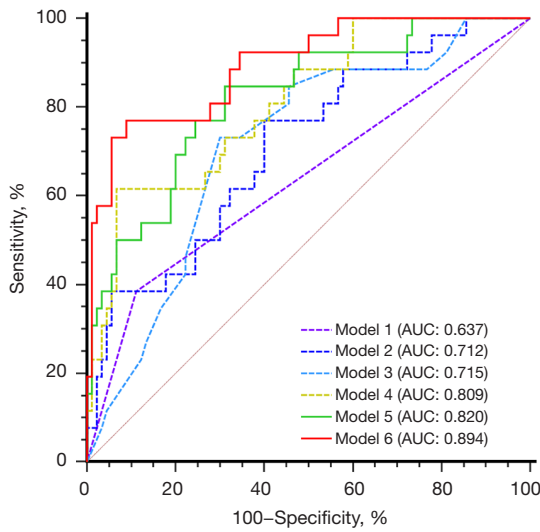


Figure 6 ROC curves for the different prediction models for MACE to measure prediction performances. The AUC of $HRP_{baseline}$, $\Delta total\ PB/year$, $FRS_{baseline}$, $\Delta PCPB/year$, $HRP_{baseline} + FRS_{baseline} + \Delta total\ PB/year$, and $HRP_{baseline} + FRS_{baseline} + \Delta PCPB/year$ were 0.637, 0.712, 0.715, 0.809, 0.820, and 0.894 ($P < 0.05$), respectively. Δ , change between baseline and follow-up. AUC, area under the curve; FRS, Framingham risk score; HRP, high-risk plaque; MACE, major adverse cardiac events; PB, plaque burden; PCPB, percent calcified plaque burden; ROC, receiver operating characteristic.

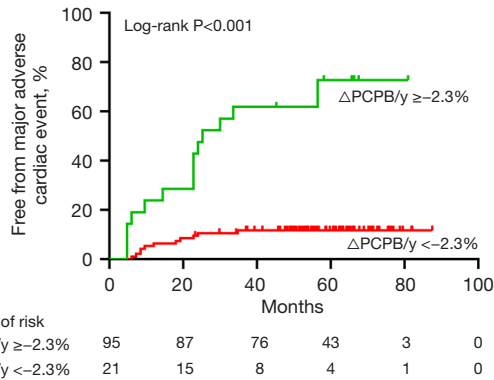


Figure 7 Kaplan-Meier survival curves for major adverse cardiac events. Δ , change between baseline and follow-up. PCPB, percent calcified plaque burden.

and noncalcification using the formula $PCPB = \text{calcified PB} / (\text{calcified PB} + \text{noncalcified PB})$. As calcification cannot decrease, if PCPB decreases, calcified PB + noncalcified PB must increase and the range of noncalcified PB increases must be greater than the range of calcified PB increases.

Conversely, the increase in the noncalcified PB must be smaller than the increase in calcified PB or it disappears. The results of this study demonstrate that $\Delta PCPB/year$ was significantly and negatively correlated with annual change of noncalcified PB, and the degree of correlation was stronger than that of the correlation with the total PB. When PCPB decreases ($\Delta PCPB/year < 0$), noncalcified PB increases significantly more than calcified PB. Conversely, the increased rate of annual change of noncalcified PB is significantly smaller than calcified PB. In the grouping from low to high according to the $\Delta PCPB/year$ quartiles, the annual change of noncalcified PB was significantly higher than calcified PB in the first two groups while the opposite result was found in the latter two groups. Therefore, while calcification is a marker of cardiovascular disease risk, an increase in PCPB is a marker of plaque stability when considered as a percentage of total PB. If PCPB decreases over time, the total PB increases, noncalcified PB increases more than calcified PB, and the plaque tends to be unstable and vice versa. Therefore, the PCPB index reflects changes in plaque composition and stability, and it may predict MACE better than the total PB.

Recently, Jin *et al.* (13) suggested that a high percentage of calcification volume at baseline CCTA is associated with a lower risk of MACE, however, they did not elucidate the predictive value of its dynamic changes. The results of this study showed that changes in PCPB had better prognostic value than baseline PCPB. Furthermore, the results demonstrate that $\Delta PCPB/year$ should replace annual change of total PB as an independent predictor of MACE and also that the prediction model constructed using $\Delta PCPB/year$ is significantly better than the total PB. When $\Delta PCPB/year$ is $< -2.3\%$, the risk of MACE increases significantly. In the univariate prediction model, the $\Delta PCPB/year$ model is better than the annual change of total PB, but there was no difference, which might be related to the relatively small sample size.

In addition to $\Delta PCPB/year$, our study showed that baseline FRS and HRP are independent predictors of MACE. Tesche *et al.* (15) also demonstrated that FRS was significantly higher in the MACE group compared with the FRS in the non-MACE group. The FRS, integrating common baseline information including gender, age and etc., has been proven to be a reliable tool for assessing the 10-year risk of cardiovascular disease events (16). In addition, HRP indicated plaque instability, which can cause acute coronary syndrome or sudden cardiac death (17-19). Tanisawa *et al.* (2) also found that the incidence of MACE in patients with

HRP was significantly higher than the incidence in patients without HRP. However, the natural course of coronary atherosclerosis was hidden. The increase or decrease of high-risk signs over time could change the nature of plaques, and predicting these changes based on baseline characteristics alone is difficult. Zhang *et al.* (20) performed serial optical coherence tomography examinations of 257 lesion segments in 72 patients and found that 25% of thin-cap fibroatheromas were transformed into fibrous plaques, and 16.7% of fibrous plaques were transformed into thin-cap fibroatheromas. Kim *et al.* (21) also suggested that decreased plaque CT values and increased high-risk signs such as punctate calcification were the pathophysiological basis of worse prognoses. The results of this study showed that the HRP, and total PB of patients in the third quartile at baseline were higher than the first two quartiles with a higher incidence of MACE. However, during the follow-up, the HRP disappeared, Δ PCPB/year increased significantly, the plaques tended to be stable, and the incidence of MACE was lower than in the former two quartiles. Therefore, a comprehensive analysis of the rich information related to the prognosis of serial CCTA and a reasonable selection of dynamic evolution indicators will greatly improve risk stratification.

Limitations

Firstly, there is a lack of verification with the gold standard intraluminal imaging for the evolution of coronary plaque, while studies have confirmed that CCTA has good feasibility in monitoring plaque evolution. Secondly, to evaluate the predictive value of PCPB for MACE, we excluded patients with normal coronary arteries or no calcified lesions, because PCPB cannot reflect the magnitude of calcification changes in these patients, and we also excluded those who underwent revascularization since surgery might affect hemodynamics and the natural course of the lesion, which might lead to selection bias. Thirdly, since this is a retrospective study, it is difficult to obtain detailed statin usage information for all patients, making it difficult to analyze the specific effects of statins on plaques. Lastly, the sample size of this study is relatively small, and this is a single-center study. Multicenter, large-sample studies are warranted to verify the clinical significance of our findings.

Conclusions

The Δ PCPB/year index derived from a series of CCTAs simultaneously reflects changes in the total and its internal compositions PB. Moreover, our study demonstrates the

potential of Δ PCPB/year to predict MACE independently from the annual change in total PB.

Acknowledgments

None.

Footnote

Reporting Checklist: The authors have completed the STROBE reporting checklist. Available at <https://qims.amegrouops.com/article/view/10.21037/qims-24-1846/rc>

Funding: None.

Conflicts of Interest: All authors have completed the ICMJE uniform disclosure form (available at <https://qims.amegrouops.com/article/view/10.21037/qims-24-1846/coif>). Y.N.D. is an employee of Siemens Healthineers Ltd., the Coronary Plaque Analysis 5.0.1 (syngo.via FRONTIER, Siemens Healthineers) equipment she provided was solely used for plaque measurement in this study. She was not involved in data analysis or interpretation of results. The other authors have no conflicts of interest to declare.

Ethical Statement: The authors are accountable for all aspects of the work in ensuring that questions related to the accuracy or integrity of any part of the work are appropriately investigated and resolved. The study was conducted in accordance with the Declaration of Helsinki (as revised in 2013). The study was approved by the Ethics Committee of The First Affiliated Hospital of Dalian Medical University (No. PJ/79-11/2019/XJS), and all patients signed an informed consent form.

Open Access Statement: This is an Open Access article distributed in accordance with the Creative Commons Attribution-NonCommercial-NoDerivs 4.0 International License (CC BY-NC-ND 4.0), which permits the non-commercial replication and distribution of the article with the strict proviso that no changes or edits are made and the original work is properly cited (including links to both the formal publication through the relevant DOI and the license). See: <https://creativecommons.org/licenses/by-nc-nd/4.0/>.

References

1. Ahmadi A, Argulian E, Leipsic J, Newby DE, Narula J.

- From Subclinical Atherosclerosis to Plaque Progression and Acute Coronary Events: JACC State-of-the-Art Review. *J Am Coll Cardiol* 2019;74:1608-17.
2. Tanisawa H, Matsumoto H, Cadet S, Higuchi S, Ohya H, Isodono K, Irie D, Kaneko K, Sumida A, Hirano T, Otaki Y, Kitamura R, Slomka PJ, Dey D, Shinke T. Quantification of Low-Attenuation Plaque Burden from Coronary CT Angiography: A Head-to-Head Comparison with Near-Infrared Spectroscopy Intravascular US. *Radiol Cardiothorac Imaging* 2023;5:e230090.
 3. Yang J, Dou G, Tesche C, De Cecco CN, Jacobs BE, Schoepf UJ, Chen Y. Progression of coronary atherosclerotic plaque burden and relationship with adverse cardiovascular event in asymptomatic diabetic patients. *BMC Cardiovasc Disord* 2019;19:39.
 4. van Rosendaal AR, Lin FY, van den Hoogen IJ, Ma X, Gianni U, Al Hussein Alawamlh O, et al. Progression of whole-heart Atherosclerosis by coronary CT and major adverse cardiovascular events. *J Cardiovasc Comput Tomogr* 2021;15:322-30.
 5. Lehmann N, Erbel R, Mahabadi AA, Rauwolf M, Möhlenkamp S, Moebus S, Kälsch H, Budde T, Schmermund A, Stang A, Führer-Sakel D, Weimar C, Roggenbuck U, Dragano N, Jöckel KH; Heinz Nixdorf Recall Study Investigators. Value of Progression of Coronary Artery Calcification for Risk Prediction of Coronary and Cardiovascular Events: Result of the HNR Study (Heinz Nixdorf Recall). *Circulation* 2018;137:665-79.
 6. Henein MY, Vancheri S, Bajraktari G, Vancheri F. Coronary Atherosclerosis Imaging. *Diagnostics (Basel)* 2020;10:65.
 7. Lee SE, Chang HJ, Sung JM, Park HB, Heo R, Rizvi A, et al. Effects of Statins on Coronary Atherosclerotic Plaques: The PARADIGM Study. *JACC Cardiovasc Imaging* 2018;11:1475-84.
 8. Soroush N, Nekouei Shahraki M, Mohammadi Jouabadi S, Amiri M, Aribas E, Stricker BH, Ahmadizar F. Statin therapy and cardiovascular protection in type 2 diabetes: The role of baseline LDL-Cholesterol levels. A systematic review and meta-analysis of observational studies. *Nutr Metab Cardiovasc Dis* 2024;34:2021-33.
 9. Yi T, Huang S, Li D, She Y, Tan K, Wang Y. The association of coronary non-calcified plaque loading based on coronary computed tomography angiogram and adverse cardiovascular events in patients with unstable coronary heart disease—a retrospective cohort study. *J Thorac Dis* 2022;14:3438-44.
 10. Liu T, Yuan X, Wang C, Sun M, Jin S, Dai X. Quantification of plaque characteristics detected by dual source computed tomography angiography to predict myocardial ischemia as assessed by single photon emission computed tomography myocardial perfusion imaging. *Quant Imaging Med Surg* 2019;9:711-21.
 11. Amann K. Media calcification and intima calcification are distinct entities in chronic kidney disease. *Clin J Am Soc Nephrol* 2008;3:1599-605.
 12. Dosseto A, Lambert K, Cheikh Hassan HI, Fuller A, Borst A, Dux F, Lonergan M, Tãcil T. Calcium isotopes as a biomarker for vascular calcification in chronic kidney disease. *Metallomics* 2023;15:mfad009.
 13. Jin HY, Weir-McCall JR, Leipsic JA, Son JW, Sellers SL, Shao M, et al. The Relationship Between Coronary Calcification and the Natural History of Coronary Artery Disease. *JACC Cardiovasc Imaging* 2021;14:233-42.
 14. Bailey G, Meadows J, Morrison AR. Imaging Atherosclerotic Plaque Calcification: Translating Biology. *Curr Atheroscler Rep* 2016;18:51.
 15. Tesche C, Plank F, De Cecco CN, Duguay TM, Albrecht MH, Varga-Szemes A, Bayer RR Nd, Yang J, Jacks IL, Gramer BM, Ebersberger U, Hoffmann E, Chiaramida SA, Feuchtner G, Schoepf UJ. Prognostic implications of coronary CT angiography-derived quantitative markers for the prediction of major adverse cardiac events. *J Cardiovasc Comput Tomogr* 2016;10:458-65.
 16. Shi H, Ge ML, Dong B, Xue QL. The Framingham risk score is associated with incident frailty, or is it? *BMC Geriatr* 2021;21:448.
 17. Munnur RK, Cheng K, Laggoune J, Talman A, Muthalaly R, Nerlekar N, Baey YW, Nogic J, Lin A, Cameron JD, Seneviratne S, Wong DTL. Quantitative plaque characterisation and association with acute coronary syndrome on medium to long term follow up: insights from computed tomography coronary angiography. *Cardiovasc Diagn Ther* 2022;12:415-25.
 18. van Assen M, von Knebel Doeberitz P, Quyyumi AA, De Cecco CN. Artificial intelligence for advanced analysis of coronary plaque. *Eur Heart J Suppl* 2023;25:C112-7.
 19. Schillaci M, Marchetti D, Andreini D. In search of new gatekeepers: coronary CT (Computed Tomography) in acute coronary syndrome. *Eur Heart J Suppl* 2023;25:B1-6.
 20. Zhang BC, Karanasos A, Gnanadesigan M, van der Sijde JN, van Ditzhuijzen N, Witberg K, Ligthart J, Diletti R, van Geuns RJ, Dijkstra J, Zijlstra F, van Soest G, Regar E. Qualitative and quantitative evaluation of dynamic changes in non-culprit coronary atherosclerotic lesion

- morphology: a longitudinal OCT study. *EuroIntervention* 2018;13:e2190-200.
21. Kim U, Leipsic JA, Sellers SL, Shao M, Blanke P, Hadamitzky M, et al. Natural History of Diabetic

Coronary Atherosclerosis by Quantitative Measurement of Serial Coronary Computed Tomographic Angiography: Results of the PARADIGM Study. *JACC Cardiovasc Imaging* 2018;11:1461-71.

Cite this article as: Wu W, Sun XX, Pan Y, Gao YQ, Dou YN, Zhang YP, Pan S, Wang H, Wang ZQ, Jia CF. Predictive value of change in percent calcified plaque burden based on serial coronary computed tomographic angiography for cardiovascular events. *Quant Imaging Med Surg* 2025;15(4):3401-3415. doi: 10.21037/qims-24-1846